AIP Journal of Applied Physics

Frequency and temperature dependence of actuating performance of Bi1/2Na1/2TiO3-BaTiO3 based relaxor/ferroelectric composites

Claudia Groh, Wook Jo, and Jürgen Rödel

Citation: Journal of Applied Physics **115**, 234107 (2014); doi: 10.1063/1.4876680

View online: http://dx.doi.org/10.1063/1.4876680

View Table of Contents: http://scitation.aip.org/content/aip/journal/jap/115/23?ver=pdfcov

Published by the AIP Publishing

Frequency and temperature dependence of actuating performance of $Bi_{1/2}Na_{1/2}TiO_3$-$BaTiO_3$ based relaxor/ferroelectric composites

Claudia Groh, Wook Jo,[a] and Jürgen Rödel
Institute of Materials Science, Technische Universität Darmstadt, Darmstadt 64287, Germany

(Received 2 February 2014; accepted 3 May 2014; published online 19 June 2014)

Recently, composites of relaxors (matrix) and either ferroelectric or nonergodic relaxor (seed) were proposed as a solution to resolving one of the main drawbacks of incipient piezoceramics, namely the requirement for high driving electric fields. In this study, we investigate the temperature and frequency dependence of the actuating performance of $Bi_{1/2}Na_{1/2}TiO_3$-$BaTiO_3$-based composites. Apart from the reduction of driving field, the composite architecture offers an extra degree of freedom for tailoring the temperature stability for different operational conditions for actuators. High strain values appear to be sensitive especially to driving frequency. This is originated by the time-dependent process of the coalescence of polar nanoregions. In effect, proximity of driving field and poling field leads to high strain sensitivity. Hence, the driving electric field needs to be adjusted in order to meet the desired frequency specifications for given applications. © *2014 AIP Publishing LLC*.
[http://dx.doi.org/10.1063/1.4876680]

I. INTRODUCTION

In the last two decades, lead-free piezoceramics have been studied in order to replace the market dominating lead zirconate titanate (PZT) in response to environmental and health concerns.[1] Recent review articles describe progresses in developing lead-free piezoceramics.[2–6] Although there is currently no lead-free material capable of replacing PZT in its versatility in applications, there are certain lead-free piezoceramics already in the market for specific applications. $Bi_{1/2}Na_{1/2}TiO_3$–$BaTiO_3$–$(Bi_{1/2}Na_{1/2})(Mn_{1/3}Nb_{2/3})O_3$ was, for example, successfully implemented in ultrasonic cleaners with a sufficient cleaning effect for commercial application.[7] For high power applications, lead-free piezoceramics were demonstrated to be superior to PZT.[8] In the field of actuator applications, there are reports on multilayer actuators (MLAs) composed of $K_{0.5}Na_{0.5}NbO_3$–based piezoceramics with Ni electrodes[9,10] and incipient piezoceramics based on $Bi_{1/2}Na_{1/2}TiO_3$–$BaTiO_3$ with Ag-Pd electrodes.[11] For the commercialization of lead-free piezoceramics, the materials themselves have to be intensively probed considering relevant application parameters (temperature and frequency stability, aging, fatigue, etc.), based on which the required properties for specific application can be steadily improved and tailored.

In the field of incipient piezoceramics, recent progress in tailoring properties has been made through 0–3 composite approaches.[12–14] The high driving electric field, required for activating large strain in incipient piezoceramics (matrix), can be reduced by blending with a nonergodic or ferroelectric phase (seed). It was further proposed that the effect is closely related to polarization coupling among the constituent phases, which leads to an inhomogeneous local field distribution, i.e., an enhanced internal electric field in the matrix as compared to that in the seed.[13,14]

MLAs often face different ambient conditions in application; for example, they are required for exhibiting good temperature insensitivity. In conventional ferroelectrics like PZT, the temperature stability is mainly limited by the Curie point T_C, where the material transforms to a paraelectric phase and is, therefore, not piezoelectrically active anymore. This is similar in nonergodic relaxors, where the ferroelectric long-range order vanishes above the ferroelectric-to-relaxor transition temperature ($T_{F\text{-}R}$).[15–17] In contrast, incipient piezoceramics are already above their transition temperature, resulting in strains which are only slightly decreasing with increasing temperature.[15] Similarly, an increasing temperature reduces the propensity for coalescing polar nanoregions (PNRs) to form a ferroelectric order and therefore requires enhanced electric fields. Therefore, the maximum achievable strain at a constant maximum electric field will decrease steadily with increasing temperature.

Another important issue for actuator applications is frequency stability. In many conventional piezoceramics, higher frequencies result in increasing coercive fields.[18–22] Similarly, in lead free relaxor ferroelectrics, the poling field—the field where the phase transformation takes places—increases with increasing frequency.[23,24] Moreover, the specific characteristics are reported to depend on the type of relaxor and the applied maximum electric field. Dittmer *et al.*[23] studied the frequency dependence of large signal properties of $(1-x)(0.81Bi_{1/2}Na_{1/2}TiO_3\text{-}0.19Bi_{1/2}K_{1/2}TiO_3)$-$xBi(Zn_{1/2}Ti_{1/2})O_3$ (hereafter, referred to as BNT-0.19BKT-xBZT) with $x = 0.02$, 0.03, and 0.04. They found that the frequency dependence of nonergodic relaxors is rather low, when the applied maximum electric field was high enough to convert the initial relaxor state fully to a ferroelectric one. However, a pronounced frequency dependence was observed at lower electric fields, where the transformation is incomplete. Similarly, a high frequency dependence was observed for ergodic relaxors. It was proposed that the frequency dependence originates from a relatively slow kinetics of

[a]Author to whom correspondence should be addressed: Electronic mail: jo@ceramics.tu-darmstadt.de

field-induced phase transition from a relaxor to a ferroelectric state.

In this paper, we reveal the effect of the composite design on the temperature and frequency dependence of incipient piezoceramics. To this end, unipolar as well as bipolar electric field loading up to an industrially acceptable maximum field of $E_{max} = 4$ kV/mm were applied to a composite comprised of a $0.91Bi_{1/2}Na_{1/2}TiO_3$-$0.06BaTiO_3$-$0.03K_{0.5}Na_{0.5}NbO_3$ as a matrix and $0.93Bi_{1/2}Na_{1/2}TiO_3$-$0.07BaTiO_3$ as a seed as a function of both temperature and frequency. It is shown that the composite design reduces the electric driving field. In addition, seed content serves as extra degree of freedom in tailoring the temperature stability to fit operational conditions.

II. EXPERIMENTAL PROCEDURE

By means of the mixed oxide route, calcined powders of the seed $0.93Bi_{1/2}Na_{1/2}TiO_3$-$0.07BaTiO_3$ and the matrix $0.91Bi_{1/2}Na_{1/2}TiO_3$-$0.06BaTiO_3$-$0.03K_{0.5}Na_{0.5}NbO_3$ were prepared. The oxides or carbonates of the respective elements, namely Bi_2O_3 (99.975% purity), $BaCO_3$ (99.8% purity), K_2CO_3 (99.0% purity), $NaCO_3$ (99.5% purity), TiO_2 (99.6% purity), and Nb_2O_5 (99.9% purity) (all Alfa Aesar GmbH & Co. KG, Karlsruhe, Germany) were mixed according to their stoichiometric formula and ball-milled in ethanol for 24 h. Calcination of the dried slurries was carried out in covered alumina crucibles for 2 h at 700 °C, followed by 3 h at 800 °C. The calcined seed powder was ball-milled for shorter time (20 min) compared to the matrix powder (24 h) in order to prevent the incorporated seed grains from being resolved in the matrix. The resulting average particle size of the seed powder (about 2 μm) was determined to be larger than that of the matrix powder (about 1 μm), from a particle-size analysis (Analysette 22 compact, Fritsch, Idar-Oberstein, Germany). To form composite samples, dried seed and matrix powders were mixed in different vol. % ratios, namely 0:100, 10:90, 20:80, 30:70, 50:50, 100:0 and processed for 30 min on a rolling bench. Pellets with a diameter of 10 mm were formed by uniaxial pressing and further compaction by a cold isostatic press at 300 MPa. Sintering was carried out at 1100 °C for 3 h in covered alumina crucibles with a heating rate of 5 K/min. The pellets were covered with an atmospheric powder of the respective compositions in order to prevent the evaporation of volatile elements during sintering. The pellets were ground down to approximately 650 μm and painted with silver paste (Gwent Group, Pontypool, United Kingdom), which was burnt in at 450 °C to form the electrodes.

Microstructure and permittivity were characterized by means of scanning electron microscopy,[25] transmission electron microscopy,[14] and temperature-dependent dielectric permittivity measurements. Despite the naturally expected diffusion during processing, characteristics of both seed and matrix are present in the composites.

Bipolar and unipolar polarization P(E) and strain S(E) hysteresis measured up to a maximum electric field of $E_{max} = 4$ kV/mm were obtained using a commercial setup (aixACCT Systems GmbH, Aachen, Germany), which is equipped with a laser interferometer. Three frequencies in the range of 500 mHz–50 Hz and six different temperatures from 25–150 °C were utilized for detailed characterization.

III. RESULTS AND DISCUSSION

A. Frequency dependence

Bipolar strain hysteresis S(E) for various composites measured at 25 °C and frequencies of 500 mHz and 5 Hz are presented in Fig. 1. The seed phase $0.93Bi_{1/2}Na_{1/2}TiO_3$-$0.07BaTiO_3$, which is a nonergodic relaxor, exhibits ferroelectric-like butterfly shaped loops, while the matrix $0.91Bi_{1/2}Na_{1/2}TiO_3$-$0.06BaTiO_3$-$0.03K_{0.5}Na_{0.5}NbO_3$, which belongs to the class of ergodic relaxors, is characterized by sprout-shaped[6] loops. The bipolar S(E) loops of the composites change gradually from sprout shape to butterfly shape with increasing seed content, consistent with earlier reports on relaxor/ferroelectric composites.[12–14] Concurrently, the electric-field-induced phase transformation changes from reversible (ergodic relaxor) to irreversible (nonergodic relaxor) with increasing seed phase. This is prominently featured by an increase in the remanent strain (S_{rem}), which arises from a persisting ferroelectric-long-range order at zero electric field.

It is known from previous publications[12–14] that in ferroelectric/relaxor composites, the poling field (E_{pol}), which is mathematically defined as the inflection point in the poling curve, is decreased with increasing seed content. This effect is present in some of our composites; while in the other composites, the poling fields lie (Fig. 1) above the maximum electric field of $E_{max} = 4$ kV/mm. Nevertheless, this effect is reflected in increasing slopes of the S(E) loops with increasing seed content. Furthermore, the poling strain (S_{pol}), which represents the strain of a virgin sample at E_{max}, is enhanced with increasing seed content.

All the ceramics investigated in this manuscript—seed, matrix, and composites—exhibit a noticeable frequency dependence, which reflects the time sensitivity of the electric-field-induced processes. Salient trends are a reduction of poling strain and a rise in poling field, where the latter is indicated by the decreasing slope of the loops presented in Fig. 1. Furthermore, E_{neg}, the electric field of highest

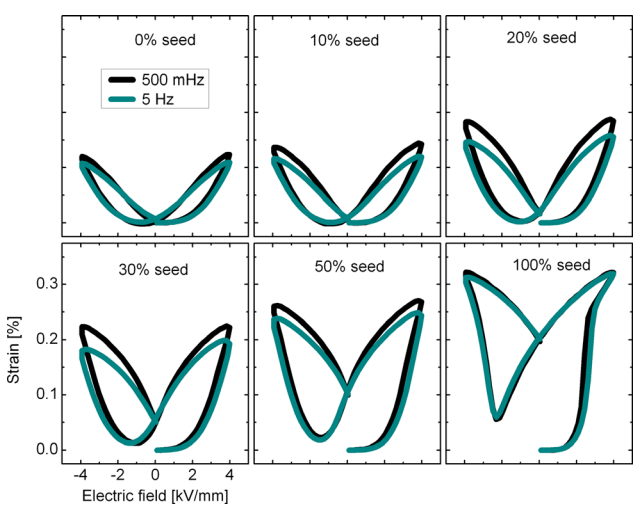

FIG. 1. Bipolar strain hysteresis for various composites, measured at frequencies of 500 mHz and 5 Hz, respectively.

negative strain, shifts to higher fields with increasing frequency. The remanent strain, S_{rem}, is rather invariant in the observed frequency range.

Similar results have been documented in other relaxors, such as lead-free BNT-0.19BKT-xBZT[23] and lead lanthanum zirconate titanate (PLZT).[26,27] In relaxor ferroelectrics in general, a lower poling strain is expected whenever the electric field is ramped up more quickly,[27] since the PNRs do have less time to coalesce and develop a ferroelectric long range order.

The impact of this effect depends strongly on the ratio between maximum and poling electric field. Similarly, in relaxor ferroelectric lead magnesium niobate lead titanate (PMN-PT), the level of the maximum electric field is reported to play an important role in the frequency-dependence of polarization and strain loops.[21,28] Whenever the electric-field level is well-above the poling field, most of the PNRs can be transformed to ferroelectric long-range order, independent of the driving frequency. In this manuscript, this is the case for the seed phase, where the applied E_{max} (=4 kV/mm) is about twice as high as the E_{pol} (~2 kV/mm). Thus, the strain achievable at the maximum electric field is virtually frequency-independent. However, at electric field levels close to the poling field, the strain is highly sensitive to the frequency, which is consistent with an earlier report on the nonergodic relaxor BNT-0.19BKT-xBZT.[23]

For the matrix, the situation is opposite; here, the maximum field is well-below the poling field. As a consequence, the shape of the strain hysteresis mimics that of an electrostrictive material.[29] Since the maximum field is below the threshold field for inducing ferroelectric long-range order, again there is only very little frequency dependence. Hence, the two end-members represent the two extreme cases, which are both rather frequency-independent: (a) mainly electrostrictive behavior with no significant phase transformation (matrix) and (b) nearly complete phase transformation (seed). In contrast, composites suffer a much stronger effect of frequency on the S(E)-loops, since here maximum electric field and poling field are of similar magnitude. Thus, the transition from relaxor to ferroelectric state is incomplete and the achievable strain depends highly on measurement frequency.

Figure 2 depicts the unipolar strain hysteresis of the composites at different frequencies. These loops are characterized in terms of normalized strain d_{33}^* (=S_{max}/E_{max}) in Fig. 3. The maximum strain achievable in the matrix can be enhanced by inserting a certain amount of seed phase, which demonstrates that the concept of relaxor/ferroelectric composites[12–14] is successfully implemented in the currently studied composites. The optimum d_{33}^* shifts from 20% seed phase at the frequency of 500 mHz to 30% seed phase at 50 Hz. This shift to higher seed contents can be rationalized as follows: At higher frequencies, the poling field increases, because the PNRs do have, compared to lower frequencies, less time to grow and develop ferroelectric long-range order. Hence, more seed phase is required for lowering the poling field. Furthermore, the frequency dependence of d_{33}^* is more pronounced for the composites as compared to that of the end-members, which is also observed in bipolar S(E) loops (see Fig. 1). As well, it is apparently related to the vicinity of maximum and poling field in the composites, as described above. The composite with 20% seed is most frequency-sensitive (about a factor of two in d_{33}^*), as the poling field is close to the maximum field.

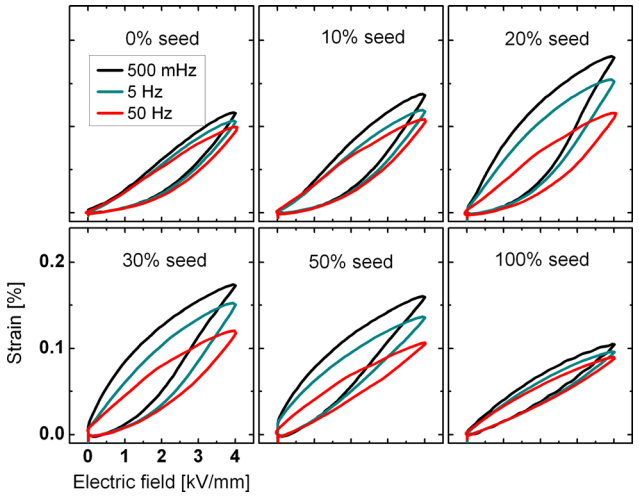

FIG. 2. Unipolar strain hysteresis for various composites, measured at frequencies of 500 mHz, 5 Hz, and 50 Hz, respectively.

B. Temperature dependence

Temperature-dependent S(E) and P(E) hysteresis of the composites measured at the frequency of 500 mHz are presented in Figs. 4(a) and 4(b), respectively. Figures 5 and 6 summarize salient parameters derived from these loops. Both increasing matrix content and increasing temperature result in a constriction in P(E) loops and an evolution of S(E) loops from butterfly to sprout shape. This is featured by a decrease of remanent polarization, P_{rem}, and coercive field, E_c, (Fig. 6), and a reduction of poling strain, S_{pol}, remanent strain, S_{rem} and negative strain, S_{neg} (Fig. 5). For nonergodic relaxors, the establishment of permanent ferroelectric long-range order is restrained above the ferroelectric to relaxor transition temperature, T_{F-R}, resulting in the absence of remanence and, therefore, sprout-shaped S(E) loops.[30–33] With T_{F-R} of the seed at 113 °C,[25] S(E) loops at 100 °C and below feature a butterfly shape, while S(E) loops at 125 °C

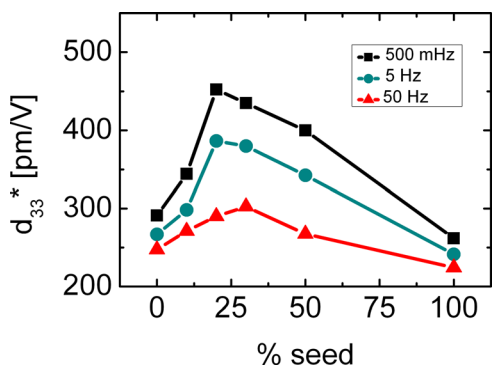

FIG. 3. Normalized strain d_{33}^* (S_{max}/E_{max}) at E_{max} = 4 kV/mm derived from unipolar strain hysteresis displayed in Fig. 2.

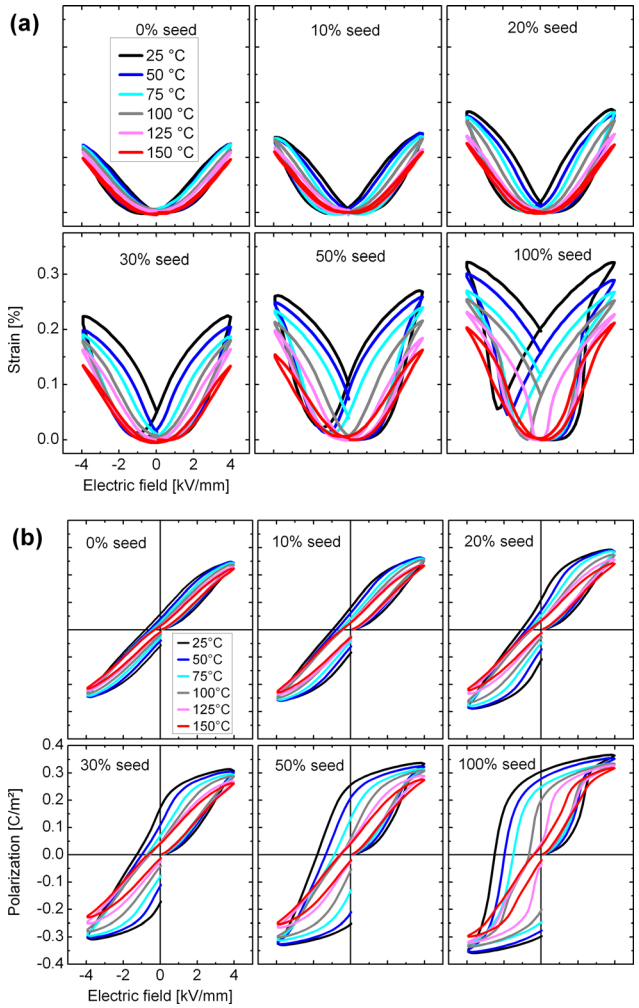

FIG. 4. Bipolar (a) strain and (b) polarization hysteresis of composites with various seed/matrix ratios measured at the frequency of 500 mHz and a temperature range of 25–150 °C.

and above are characterized by a sprout shape. The matrix, which belongs to the class of ergodic relaxors is at room temperature already above its $T_{F\text{-}R}$ and will, therefore, establish no significant permanent ferroelectric long-range order, resulting in a sprout-shaped S(E) loop at 25 °C. Upon increasing temperature from room temperature up to 150 °C, there is no change in the shape of the S(E) loop. This is typically seen for ergodic relaxors,[30–32] which feature their highest strains in the vicinity of $T_{F\text{-}R}$.[6,34]

For the composites, temperature-dependent remanent strain merges at a single temperature, $T_{F\text{-}R\_seed}$ (see Fig. 5(d)). This is consistent with the temperature-dependent

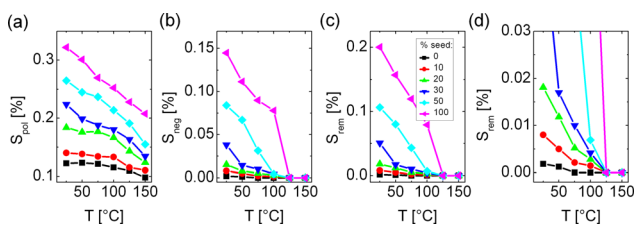

FIG. 5. (a) S_{pol}, (b) S_{neg}, and (c) S_{rem} as function of temperature as derived from the bipolar strain hysteresis shown in Fig. 4(a). A magnified view of S_{rem} is displayed in Fig 5(d).

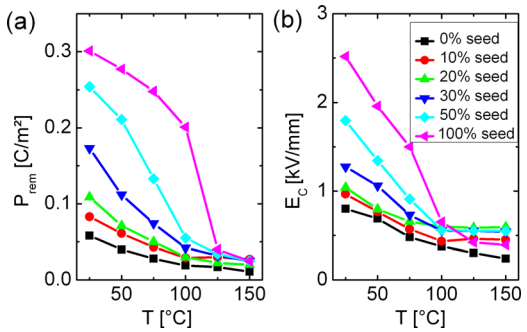

FIG. 6. (a) P_{rem} and (b) E_c derived from the bipolar polarization hysteresis provided in Fig. 4(b).

dielectric permittivity measurement from our previous report, where no archetypical $T_{F\text{-}R}$ was observed for the composites; although the difference between poled and unpoled dielectric permittivity converged at $T_{F\text{-}R\_seed}$.[25] The successful formation of composite with two distinct phases is therefore reflected in both, large signal and small signal measurements.

Figure 7 presents a contour plot of the normalized strain d_{33}* of composites as a function of temperature and seed content, based on measurement data of composites with 0, 10, 20, 30, 50, and 100% seed content at temperatures of 25, 50, 75, 100, 125, and 150 °C. As expected from bipolar S(E) loops, the pure matrix material offers a stable strain in the investigated temperature range; however, the strain is rather low in comparison to the composites. The seed phase exhibits little strain at room temperature, which enhances drastically with increasing temperature and reaches its maximum in the vicinity of $T_{F\text{-}R}$ (113 °C). This represents the temperature where the transformation from a nonergodic relaxor to an ergodic relaxor takes place. This implies that the phase transformation shifts from irreversible to reversible, respectively; and therefore, no remanence is present anymore. For the composites there is no archetypical $T_{F\text{-}R}$, however, the remanence decreases with increasing temperature and increasing matrix content as seen in Figs. 5(c)–6(a). This is in good accordance

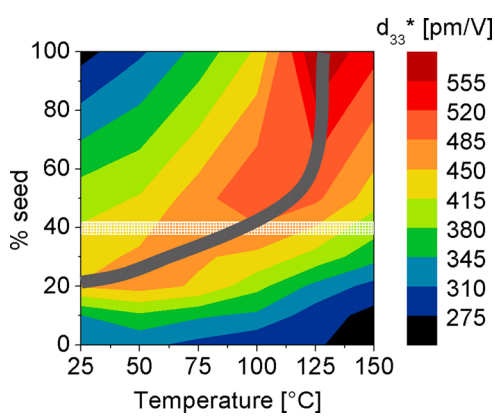

FIG. 7. Normalized strain d_{33}* (=S_{max}/E_{max}) for composites with different seed contents and temperatures measured at a frequency of 500 mHz. At 40% seed content, the best temperature stability paired with high strain is expected (white shaded area in the plot). Furthermore, the solid grey line represents a guide for the eye of maximum strain in temperature and composition space.

with the solid grey line in Fig. 7, which provides a guide for the eye for the optimum d_{33}* in a space spanned by temperature and seed content. In the investigated temperature range of 25–150 °C, the best temperature stability combined with high strain is expected at about 40% seed content in the composites, as highlighted by a white shaded box in Fig. 7.

In the same temperature range, conventional PZT, which is widely used in actuator applications, exhibits a smaller temperature sensitivity of d_{33}*.[35] In detail, the evolution of normalized strain with temperature depends on the position of the material with respect to the morphotropic phase boundary.

For the composites, it is noted that a small amount of strain at room temperature has to be sacrificed in order to improve temperature stability over the entire investigated temperature range. The composite providing the highest strain at room temperature (20% seed content) displays, in comparison to the composites with best temperature-stability (40% seed content), a higher temperature sensitivity, especially at temperatures above 100 °C. Consequently, it is important to define the conditions the actuator has to face during operation in order to tailor the properties of the composites according to the specific needs.

C. Temperature and frequency-dependence

A comparison of frequency dependence of bipolar S(E) loops at 25 and 100 °C, respectively, is provided in Fig. 8. As mentioned above, the shapes of the loops develop from butterfly loops at room temperature to sprout-shaped loops at higher temperatures (see also Fig. 4(a)). Figure 8 reveals that the loops at 100 °C, which mimic the ones of electrostrictive materials, are rather frequency-independent, which is in good agreement with the frequency-insensitive electrostrictive-like loops of the pure matrix at 25 °C. In contrast, bipolar S(E) loops of composites at 25 °C present a considerable influence of measurement frequencies, since the maximum electric field is in the vicinity of E_{pol}, where the time-dependent phase transformation takes place. Thus, an increase in frequency, and therefore a reduction of the

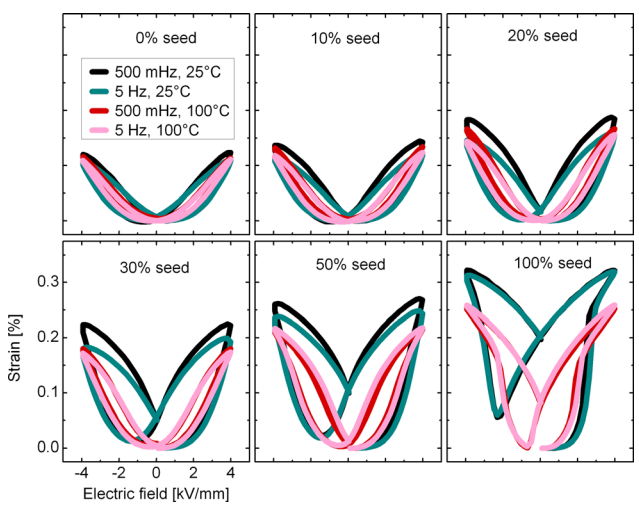

FIG. 8. Bipolar S(E) of composites with varying seed contents measured at frequencies of 500 mHz and 5 Hz and temperatures of 25 and 100 °C.

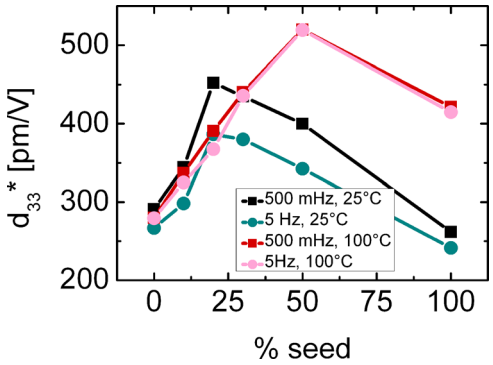

FIG. 9. Normalized strain d_{33}* (=S_{max}/E_{max}) of composites with varying seed content measured at frequencies of 500 mHz and 5 Hz and temperatures of 25 and 100 °C.

allotted time for the phase transformation from relaxor to ferroelectric phase, results in a pronounced decrease of strain response (*cf.* Sec. I). At high temperatures, one of the salient trends at room temperature, the reduction of poling strain with increasing frequency, diminishes. Also, the increase in poling field is less pronounced. This mitigated frequency dependence at higher temperatures may be due to enhanced kinetics, which eases the phase transformation from relaxor to ferroelectric phase and *vice versa*.

Furthermore, the frequency dependence of the pure seed at 100 °C seems to be slightly reduced. This might be due to a reduction of poling field, E_{pol}, at higher temperatures which eases the coalescence of PNRs at low electric fields and therefore enforces the complete transformation to ferroelectric long range order at the maximum electric field, E_{max}, which provides enhanced frequency insensitivity.

Figure 9 displays the frequency dependence of normalized strain d_{33}* measured at 25 °C and 100 °C, respectively. As described in Sec. II, the maximum of d_{33}* shifts to higher seed contents with increasing temperature. At room temperature, the maximum in d_{33}* is obtained at 20% seed phase; while at 100 °C, the maximum is at 50% seed phase. The pronounced frequency dependence of d_{33}* at room temperature, which is related to the slow kinetics of the electric-field-induced phase transformation (*cf.* Sec. I), is strongly diminished at 100 °C. This is in good agreement with the mitigated frequency dependence of corresponding bipolar S(E) loops at high temperatures (Fig. 8).

IV. CONCLUSIONS

The actuating performance of $Bi_{1/2}Na_{1/2}TiO_3$-$BaTiO_3$-based composites was tailored by adapting the seed content in order to meet the needs for specific applications. We demonstrated that the currently adopted composite approach is beneficial not only in tailoring strain properties but also in tuning the temperature stability of strains. In the current investigation, the highest strain at room temperature is offered by a composite containing 20% seed phase, while the best temperature stability in the investigated range of 25–150 °C is expected for a composite comprised of 40% seed phase.

A pronounced frequency dependence of the composites, compared to the constituent phases, is found which can be

rationalized by the vicinity of maximum electric field E_{max} to the poling field E_{pol}. Since the process of coalescing PNRs is highly time-dependent, the poling field and therefore also the amount of giant strain generated depend on the driving frequency. Therefore, (a) the achievable strain is strongly frequency-dependent and (b) this frequency dependence is reduced at higher temperatures due to enhanced phase transformation kinetics. For a specific application, it is important to adjust the maximum electric field according to the specific frequency range.

ACKNOWLEDGMENTS

The work was supported by the Hesse state center AdRIA on adaptronics. The authors wish to thank Dr. Soon-Jong Jeong for helpful discussion.

[1]Off. J. of Eur. Union **54** [L174], 88 (2011).
[2]E. Aksel and J. L. Jones, Sensors **10**, 1935 (2010).
[3]D. Damjanovic, N. Klein, J. Li, and V. Porokhonskyy, Funct. Mater. Lett. **3**, 5 (2010).
[4]J. Rödel, W. Jo, K. T. P. Seifert, E.-M. Anton, T. Granzow, and D. Damjanovic, J. Am. Ceram. Soc. **92**, 1153 (2009).
[5]T. Takenaka, H. Nagata, and Y. Hiruma, Jpn. J. Appl. Phys., Part 1 **47**, 3787 (2008).
[6]W. Jo, R. Dittmer, M. Acosta, J. Zang, C. Groh, E. Sapper, K. Wang, and J. Rödel, J. Electroceram. **29**, 71 (2012).
[7]T. Tou, Y. Hamaguti, Y. Maida, H. Yamamori, K. Takahashi, and Y. Terashima, Jpn. J. Appl. Phys., Part 1 **48**, 07GM03 (2009).
[8]Y. Doshida, H. Shimizu, Y. Mizuno, and H. Tamura, Jpn. J. Appl. Phys., Part 1 **52**, 07HE01 (2013).
[9]S. Kawada, M. Kimura, Y. Higuchi, and H. Takagi, Appl. Phys. Express **2**, 111401 (2009).
[10]K. Kobayashi, C. A. Randall, M. Ryu, Y. Doshida, and Y. Mizuno, in 2012 Joint 21st IEEE ISAF/11th IEEE ECAP/IEEE PFM (ISAF/ECAPD/PFM), Aveiro, Portugal, 2012.
[11]W. Krauss, D. Schutz, M. Naderer, D. Orosel, and K. Reichmann, J. Eur. Ceram. Soc. **31**, 1857 (2011).
[12]D. S. Lee, D. H. Lim, M. S. Kim, K. H. Kim, and S. J. Jeong, Appl. Phys. Lett. **99**, 062906 (2011).
[13]D. S. Lee, S. J. Jeong, M. S. Kim, and J. H. Koh, J. Appl. Phys. **112**, 124109 (2012).
[14]C. Groh, D. J. Franzbach, W. Jo, K. G. Webber, J. Kling, L. A. Schmitt, H.-J. Kleebe, S.-J. Jeong, J.-S. Lee, and J. Rödel, Adv. Funct. Mater. **24**, 356 (2013).
[15]W. Jo, S. Schaab, E. Sapper, L. A. Schmitt, H.-J. Kleebe, A. J. Bell, and J. Rödel, J. Appl. Phys. **110**, 074106 (2011).
[16]L. Pardo, E. Mercadelli, Á. García, K. Brebøl, and C. Galassi, IEEE Trans. Ultrasonics, Ferroelectr., Freq. Control **58**, 1893 (2011).
[17]W. Ge, C. Luo, C. P. Devreugd, Q. Zhang, Y. Ren, J. Li, H. Luo, and D. Viehland, Appl. Phys. Lett. **103**, 241914 (2013).
[18]N. Lee and S.-J. Kim, Ceram. Int. **38**, 1115 (2012).
[19]M. H. Lente, J. Appl. Phys. **95**, 2646 (2004).
[20]Y. Gao, K. Uchino, and D. Viehland, J. Appl. Phys. **92**, 2094 (2002).
[21]Y. H. Chen and D. Viehland, Appl. Phys. Lett. **77**, 133 (2000).
[22]D. Zhou, M. Kamlah, and D. Munz, Proc. SPIE **4333**, 64 (2001).
[23]R. Dittmer, W. Jo, E. Aulbach, T. Granzow, and J. Rödel, J. Appl. Phys. **112**, 014101 (2012).
[24]A. J. Royles, A. J. Bell, J. E. Daniels, S. J. Milne, and T. P. Comyn, Appl. Phys. Lett. **98**, 182904 (2011).
[25]C. Groh, W. Jo, and J. Rödel, J. Am. Ceram. Soc. **97**, 1465 (2014).
[26]Z. Y. Meng, U. Kumar, and L. E. Cross, J. Am. Ceram. Soc. **68**, 459 (1985).
[27]Q. M. Zhang, S. J. Jang, and L. E. Cross, J. Appl. Phys. **65**, 2807 (1989).
[28]D. Viehland and Y.-H. Chen, J. Appl. Phys. **88**, 6696 (2000).
[29]S.-T. Zhang, A. B. Kounga, W. Jo, C. Jamin, K. Seifert, T. Granzow, J. Rödel, and D. Damjanovic, Adv. Mater. **21**, 4716 (2009).
[30]K. T. P. Seifert, W. Jo, and J. Rödel, J. Am. Ceram. Soc. **93**, 1392 (2010).
[31]K. Wang, A. Hussain, W. Jo, and J. Rödel, J. Am. Ceram. Soc. **95**, 2241 (2012).
[32]S.-T. Zhang, A. B. Kounga, E. Aulbach, W. Jo, T. Granzow, H. Ehrenberg, and J. Rödel, J. Appl. Phys. **103**, 034108 (2008).
[33]C. Xu, D. Lin, and K. W. Kwok, Solid State Sci. **10**, 934 (2008).
[34]H. Jigong, B. Wangfeng, L. Wei, S. Bo, and Z. Jiwei, J. Appl. Phys. **114**, 044103 (2013).
[35]H. Kungl and M. J. Hoffmann, Acta Mater. **55**, 5780 (2007).